Reconnection of multiple scroll rings in a three-dimensional reaction-diffusion system

Dhriti Mahanta and Sumana Dutta*
Department of Chemistry, Indian Institute of Technology Guwahati, Guwahati 781039, India

(Received 23 May 2019; published 27 August 2019)

Two scroll rings, placed in close proximity, can interact. When they come within one core length of each other, these waves can reconnect to form a single, large filament. In this article we show that three or more scroll rings can also reconnect when they come within the critical distance. Multiple scroll rings form larger vortices of varied filament geometry, depending on their initial sizes and placements. Different filaments, resulting from a reconnection of the same number of scroll rings placed in diverse ways, can have different lifetimes. In experiments with the Belousov-Zhabotinsky reaction and numerical simulations based on a corresponding reaction-diffusion model, we demonstrate the interaction and reconnection of multiple scroll waves and try to elucidate their lifetimes and dynamics.

DOI: 10.1103/PhysRevE.100.022222

I. INTRODUCTION

Chemical waves have been the subject of extensive theoretical and experimental investigations in recent decades as they form an integral part of nonlinear phenomena occurring in systems far from thermodynamic equilibrium. Specific chemical reactions coupled with diffusion give rise to waves and patterns that are similar to those widely encountered in various systems spreading across biology, physics, ecology, sociology, economics, medicine, and many other disciplines [1,2]. Among them are the two-dimensional (2D) spirals and their three-dimensional analogs, the scroll waves [3]. These are found in excitable chemical media as well as in many biological systems such as chicken retina [4], mammalian neocortex [5], frog oocytes [6], colonies of *Dictyostelium discoideum* [7], and the myocardium of the heart [8]. The propagation of these waves in the heart tissue has been suggested to be linked with abnormal cardiac rhythms, a condition referred to as cardiac arrhythmia. Some of the cardiac arrhythmias are life threatening and may even lead to the death of the patient within minutes [9,10]. The studies of spiral and scroll waves in chemical media are often motivated by their occurrence in the cardiac system and the role they play in cardiac arrest. Extensive experimental and numerical studies have been carried out on the spiral waves; however, the same cannot be said for the three-dimensional scrolls. Though numerical and analytical works on scroll wave dynamics have been reported since the 1980s [11,12], they are relatively less explored in experimental systems, perhaps due to the difficulties in visualizing the actual dynamics in the interior of a thick system. Some chemical systems, like the Belousov-Zhabotinsky (BZ) reaction, have emerged as the simplest table-top models of wave propagation in cardiac tissue [13].

Three-dimensional scroll waves rotate around one-dimensional curves, called filaments [14]. Early theoretical works on scroll waves and their filaments suggest that any nonintersecting closed curve of arbitrary shape evolves toward a circle and disappears in finite time [15,16]. It has been established by these mathematical studies that temporal evolution of a filament occurs according to local speeds that are functions of the local curvatures:

$$\frac{d\mathbf{s}}{dt} = \alpha\kappa\hat{\mathbf{N}}, \tag{1}$$

where $\mathbf{s}$ is the one-dimensional curve, α describes a system-specific constant line tension, κ is the local curvature, and $\hat{\mathbf{N}}$ denotes the curve's unit normal vector [12]. If α is negative, then the scroll would evolve as an expanding circle. When α is positive, we say the filament has positive tension and it shrinks with time, which is seen in the case of the BZ scroll wave.

The dynamics of the filaments can be controlled using external field gradients [17,18]. It has been shown that a thermal or electric gradient can reorient a filament and can even reverse spontaneous filament shrinkage. A scroll wave filament can also be affected by another neighboring filament [19,20]. Since in a natural system there could be many such filaments lying in close proximity, the study of scroll wave interaction would be very interesting and reveal crucial information regarding the propagation and control of reentrant waves in the myocardial tissue. Although the interaction of spiral waves in 2D systems is a well-studied phenomenon [21–23], there have been very few experimental reports of scroll wave interaction, and many facets of the latter still remain unexplored. Theoretical studies of interacting filaments suggest that two filaments can undergo crossover collision when they fall within one core length of each other [24]. The effect of such interactions on the lifetime of the neighboring scroll rings has also been investigated in yet another computational study [25]. Numerical simulations of filament interaction in the ventricular wall suggests the appearance of complex activation patterns on the surface of the heart [26]. However, the effect of such interaction on the dynamics and lifetime of the reconnected filament has not been addressed in these investigations.

*sumana@iitg.ac.in

In the experimental BZ system, interaction between a pair of straight, parallel scroll waves was investigated using optical tomography technique by Hauser and coworkers in 2013 [19], where they demonstrated the repulsion and synchronization of the filaments. In a recent study, we have shown how the interaction between a pair of scroll rings having circular filaments may lead to either reconnection or repulsion depending on whether they have the same or opposite sense of rotation [20]. This was the first-ever experimental demonstration of scroll wave reconnection. Two coplanar scroll waves can undergo crossover collision, and they can reconnect to form a much larger filament, when they are within a critical distance of each other. In contrast, when the distance between the filaments is more than the critical distance, the two scroll rings rotate independently, and their interfilament distance goes on increasing, as they shrink with time. Thus the filaments can reconnect only within a very specific range of initial wave distances. This distance is equal to the length of a rotor core. However, in these earlier studies, the filament dynamics of the reconnected scroll waves were not investigated in detail. It would be interesting to see the effect of the reconnection on the lifetimes of the newly formed scrolls. Also, so far, only two interacting scroll waves have been studied. The more complicated scenario of multiple scroll wave interaction is worth investigating.

In the current manuscript, we report the results of a detailed investigation on the interaction of multiple coplanar scroll rings placed in close vicinity of one another. We show that within the specific range of inter filament distances, the scroll rings reconnect to form larger scrolls of complex geometries. The filaments then undergo reshaping over time and shrink under a medium-specific positive filament tension. We carry out experiments with the BZ system to study the interaction of three to six scroll waves. By changing the arrangement of the scroll rings for a particular number of interacting filaments, we investigate the change in the resulting reconnection. We further explore the dynamics and lifetime of the various reconnected filaments in detail. Numerical studies have been performed using the Barkley model to better understand the filament dynamics in three dimensions.

II. EXPERIMENTAL METHODS

We used the gel-immobilized ferroin-catalyzed BZ reaction for performing our experiments. The reaction was carried out in a Petri dish using two BZ gel layers. Each layer had a thickness of 4 mm. The concentrations of all the chemicals were identical in both the gel layers consisting of 0.8% (w/v) agarose. The initial concentrations of the reactants were taken as $[NaBrO_3] = 0.04$ M, $[CH_2(COOH)_2] = 0.04$ M, $[H_2SO_4] = 0.16$ M, and $[Fe(o\text{-}phen)_3SO_4] = 0.5$ mM. In this concentration range, the scroll waves have positive filament tension [27] which implies a gradual shrinkage of the free scroll rings and their disappearance in finite time. All solutions and gels were prepared in ultrapure water with a resistivity of 18.2 MΩ cm . The experiments were carried out at room temperature ($22 \pm 1\,^{\circ}$C).

For studying the reconnection of n number of scroll waves ($n \geqslant 3$), the tips of equal number of clean silver wires, of diameter 0.5 mm each, were simultaneously inserted into the bottom gel layer for a few seconds. Metallic silver decreases the local concentration of the inhibitory Br^- ion, thus leading to the creation of n expanding chemical waves. When the waves reached the desired dimensions, the second layer was poured over the system. Special care was taken so that the nearest distances between any two neighboring waves, and consequently the resulting filaments, were nearly identical and within the range where reconnection can occur [20]. Subsequently, the rim of each of the semispherical waves in the lower layer curled up into the upper gel layer and gave rise to a circular scroll ring. The system was illuminated by a cold white light from below. The reaction was monitored with a charge-coupled-device camera equipped with a blue dichroic filter mounted above the Petri dish. The top view of the reaction chamber (640 × 480 pixels) was recorded at 2-s intervals. The resulting time-lapse images were finally analyzed using in-house MATLAB scripts.

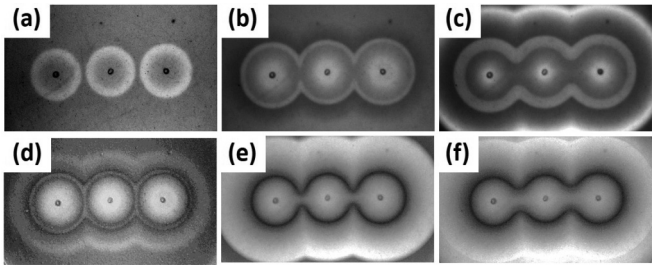

FIG. 1. Reconnection of three scroll waves whose centers lie on a straight line: [(a)–(c)] Snapshots of the reaction chamber at time intervals of 7 min. [(d)–(f)] Reconstructed filaments corresponding to the snapshots in the top panel, calculated over one time period. The dark areas of singularity show the position of the filaments. Area of each snapshot is 3.9 cm × 2.3 cm. The rings are of diameters 9.84, 9.54, and 10.23 mm (from the left to right) and inter-ring distances are 1.1 and 1.1 mm, respectively. See the Supplemental Material for movies [28].

III. EXPERIMENTAL RESULTS

Figure 1 shows the result of a typical experiment, where three independent scroll rings placed side by side reconnect. In Figs. 1(a)–1(c), the top views of the experiment, during the first three rotations of the scrolls, are shown. The corresponding filaments reconstructed with the help of a MATLAB code are depicted in the second column [Figs. 1(d)–1(f)]. The intense black curves represent the filament. The initial diameters of the three circular filaments (d_0) are in the range of 9.54 to 10.21 mm. The waves are nearly uniformly spaced, with the separation distance being 1.1 mm. The scrolls undergo one rotation individually [Fig. 1(a)], and then during the next cycle of rotation, the middle ring reconnects at one point on its either side, with the two neighboring rings [Fig. 1(b)]. The three independent circular filaments are seen in Fig. 1(d), which attract each other and merge to form one large filament in Fig. 1(e). After reconnection, the bottlenecks in the newly formed filament start to expand slowly [Fig. 1(f)] under the curvature-dependent motion. The filament eventually approaches a hot dog–like shape as it slowly shrinks and finally disappears.

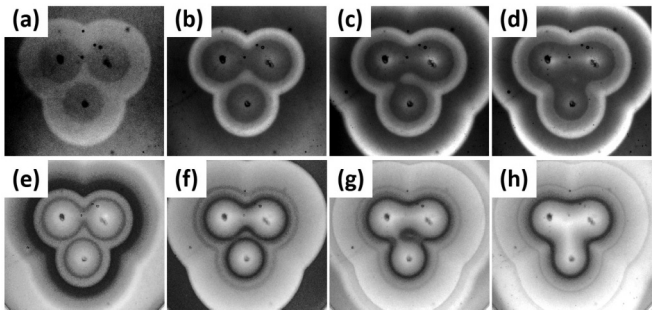

FIG. 2. Crossover collision of three scroll rings whose centers trace an equilateral triangle: [(a)–(d)] Snapshots of the experiment, with a time interval of 7 min between two consequent snapshots. [(e)–(h)] Filaments corresponding to the snapshot above it, calculated over one time period. The area of each snapshot is 3.3 cm × 3.1 cm. The sides of the equilateral triangle (intercenter distance) are 0.99 cm in length. The rings are of diameter sizes 9.74, 9.54, and 9.15 mm (clockwise from the top left) and inter-ring distances are 0.2, 0.51, and 0.51 mm, respectively. See the Supplemental Material for movies [28].

We then placed three scroll rings, of sizes comparable to that in the previous experiment (diameter range 9.15 to 9.74 mm), in a triangular fashion. Figure 2 shows the results of one such experiment. Here the two semispherical waves placed side by side had an initial separation of ∼0.2 mm. The smallest distance between the third ring to these two rings are about 0.51 mm. These information can be gathered from the snapshot of the waves before pouring in the second layer. After the initiation of the experiment, the first rotation [Figs. 2(a) and 2(e)] shows that the two circular waves which were very closely spaced, emerged as a single scroll wave, with a dumbbell shape and a very thin belly. The third wave, which had an appreciable distance from these two, undergoes independent rotation as a scroll ring. In the second period [Fig. 2(b)], these two filaments (dumbbell shaped and circular) again undergo distinct rotations. However, the filaments are now closer than before [Fig. 2(f)]. In the next period, the small scroll wave connects to the left lobe of the dumbbell [Fig. 2(c)], followed by the right lobe during the fourth rotation [Fig. 2(d)]. The final reconnected filament [Fig. 2(h)] is trefoil shaped. The shape of this filament is, however, distinctly different from the trefoil knots that have been extensively studied in earlier theoretical works [29].

A similar experiment was carried out for three initial waves having diameters 11.02, 11.41, and 11.32 mm, and interwave distances 1.16, 1.52, and 1.52 mm [28]. Three circular scroll rings were formed, and they all remained disconnected, even after several time periods. It was observed that they carried out individual rotations as they eventually shrunk and disappeared.

We designed and carried out several more experiments involving four, five, and six scroll rings and found successful filament reconnection whenever any two filaments were separated by a distance shorter than 1.1 mm (one core length). An experiment with six scroll rings is depicted in Fig. 3. Since this experiment requires the initiation of six scroll rings simultaneously, it is experimentally very challenging to maintain similar sizes and equal distances between the scroll rings. The initial condition in this experiment is six circular waves [Fig. 3(a)], with diameters ranging between 8.86 and

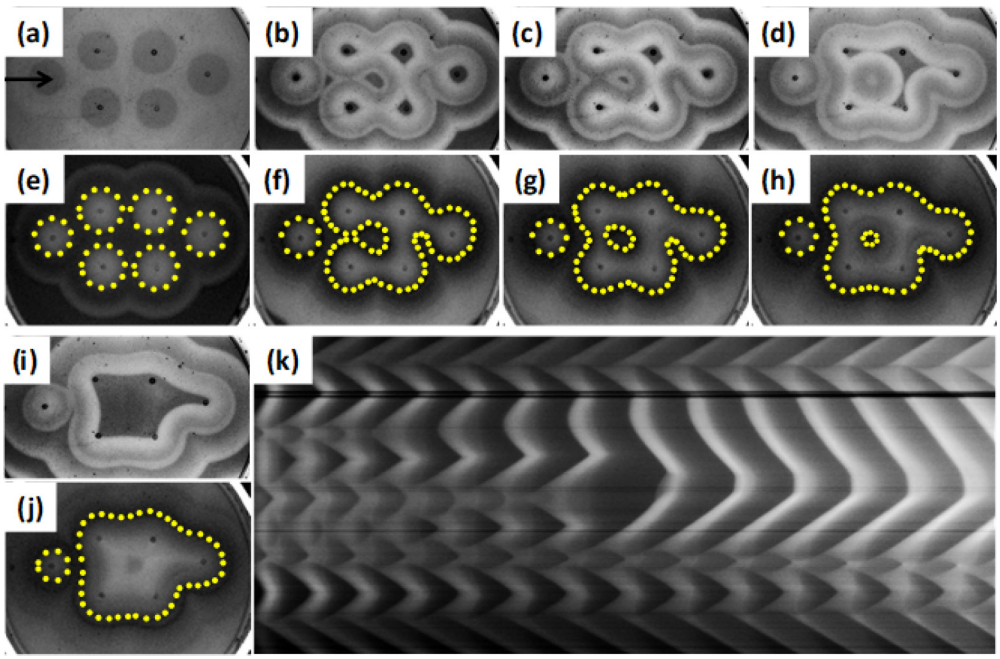

FIG. 3. Interaction dynamics of six scroll waves placed in close proximity. [(a)–(d) and (i)] Snapshots of the experiment at (a) 3, (b) 17, (c) 24, (d) 38, and (i) 52 min after scroll-wave initiation. Each snapshot covers an area of 5.7 cm × 3.4 cm. The filaments over one time period corresponding to the snapshots are shown in the following row [(e)–(h) and (j)]. The (yellow) dotted lines are the reconstructed filaments. (k) Time-space plot reconstructed along the small black arrow shown in (a). Time increases from left to right. See the Supplemental Material for movies [28].

10.43 mm. Details of all sizes and distances marked in the snapshot just before pouring in the second gel layer is given in Ref. [28] (supplementary Fig. 1). The nearest distances between the circles vary from 0.51 to 2.03 mm. During the first rotation, the six circular filaments can be independently discerned [Fig. 3(e)]. After the second rotation, most of these rings can be seen to have already reconnected to form a single large filament [Figs. 3(b) and 3(f)], except the one on the far left. The initial distances of this latter wave from its two nearest neighbors were 1.27 and 2.03 mm, respectively. As a result, this wave fails to reconnect with either of its neighbors. Another interfilament distance which was greater than 1.1 mm (core size of a spiral) was that between the rightmost ring and its next neighbor (moving clockwise). It can be observed that around this area, the two filaments continue to rotate independently for about half a dozen rotations, until the curvature-dependent motion of the large reconnected filament finally smoothes out the curves [Figs. 3(i) and 3(j)]. Meanwhile, another interesting observation was made. In Fig. 3(g), one can find a small circular filament embedded within the newly formed large, reconnected filament. This filament was also formed as a result of the reconnection of the four circular rings around the area where it was born. This circular filament, due to its small size, rapidly shrinks and disappears very quickly [Figs. 3(h) and 3(j)]. Figure 3(k) depicts the time-space plot of the experiment. Initially there are six independent scroll rings, which gives a fairly complicated pattern. However, if one traces the number of times a line drawn along the black arrow in Fig. 3(a) cuts through filaments, then the number is initially eight and eventually reduces to seven, six, five, and, finally, four. If we look at the filament in Fig. 3(g), then a horizontal line in the middle would come across eight filament segments, while in Fig. 3(j), the same line will cut across such filament segments only four times.

IV. NUMERICAL SIMULATIONS

We carried out numerical simulations using the three-dimensional Barkley model [30]. This two-variable activator-inhibitor system is often used for modeling reaction-diffusion systems in general, and the BZ reaction in particular [31],

$$\frac{\partial u}{\partial t} = \frac{1}{\epsilon}\left\{u(1-u)\left(u - \frac{v+b}{a}\right)\right\} + D_u\nabla^2 u,$$
$$\frac{\partial v}{\partial t} = u - v + D_v\nabla^2 v.$$

In the BZ system, the fast variable u and the slow variable v of the Barkley model qualitatively relate to the concentrations of $HBrO_2$ and ferroin, respectively. Our simulations were carried out in a three-dimensional space sized $800 \times 800 \times 450$ grid points, having zero flux boundary conditions along all edges. The differential equations were numerically integrated using the fourth-order Runge Kutta scheme and a 19-point Laplacian stencil. The integration time step was kept constant at 0.012 and the lattice grid spacing was maintained at 0.35. The values of the system parameters were taken as $a = 0.84$, $b = 0.07$, $\epsilon = 0.02$ and diffusion constants are $D_u = D_v = 1.0$. This set of parameters was chosen because it showed negligible drift of the scroll in binormal direction and positive filament tension, as is seen in our experiments. The filaments of the scroll waves were identified as regions where $u = 0.5$ and $v = a/2 - b$.

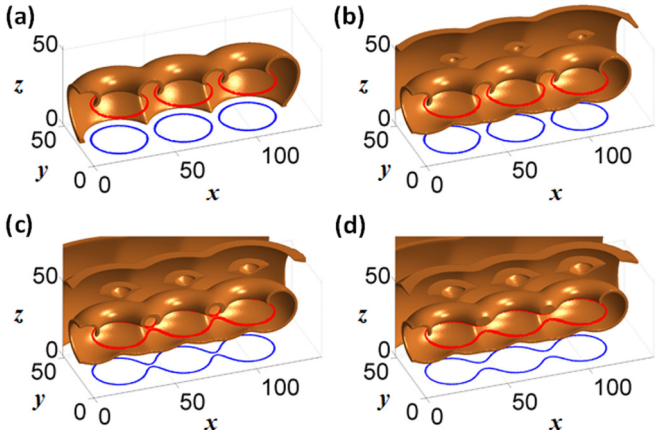

FIG. 4. Numerical simulation of the reconnection of three scroll waves arranged in a linear fashion. The wave patterns are seen as solid brown areas. The red curves are the filaments. The two-dimensional projections of the filaments are shown in blue at the bottom of the box ($z = 0$). Time interval between each pair of successive frames is 5.4 time units. The computed volume has been cropped along the boundaries in these images.

The simulations were initiated just like the experiments. Figure 4 depicts the case where three scroll rings, placed horizontally with their centers falling on a line, merge to form a large reconnected scroll wave. This mimics the experiment demonstrated in Fig. 1. Here three small, spherical waves were started from three collinear, equidistant points. When the waves reached desired dimensions, we annihilated their top halves. At this instant each circular wave had a diameter of 35.7 space units and the distance between two neighboring waves was 4.1 space units. Each semispherical wave then curled up into the layer on top of it and formed an independent scroll ring [Fig. 4(a)]. The filaments (red curves in Fig. 4) are sufficiently close to interact with each other and with time they begin to attract at the points of nearest approach, as seen in Fig. 4(b). They eventually reconnect at these two points and give rise to a single large filament [Fig. 4(c)] that remains in the same plane, as the initial waves. The latter then slowly smooths out its curves, as it shrinks under curvature flow motions [Fig. 4(d)]. This figure also shows the excitation waves as solid brown areas ($v > 0.4$). Only the rear half of the waves are shown here for the sake of clarity. Initially, these waves undergo rotatory motion around the three filaments and are eventually drawn closer to join at the points where the filaments undergo reconnection.

In another simulation, we initiated three scroll rings in a manner so that their centers fall on the vertices of an equilateral triangle, like the experiment in Fig. 2. In Fig. 5 we show the filament dynamics of the system during the first eight rotation periods. Initially the three filaments are disconnected, though a considerable attraction can be seen to be acting on them at the three points [Fig. 5(a)] of nearest approach, where the filaments become slightly pointy. In the next rotation, they approach each other and almost touch

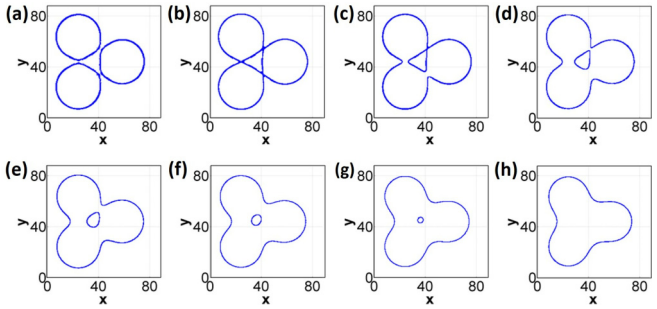

FIG. 5. Filament dynamics of the reconnection of three circular filaments whose centers trace an equilateral triangle. The first eight rotation cycles of the filaments are shown as viewed from the top. Time interval between subsequent frames is 5.4 time units. The diameter of the initial waves are 35.7 space units and they are separated from one another by a distance of 4.1 space units at the points of nearest approach.

at these three points [Fig. 5(b)]. During the third rotation, one of the filaments reconnects with the other two, forming a single, large filament [Fig. 5(c)]. This is followed by a reconnection at the third point of approach [Fig. 5(d)]. Here one may observe the formation of a large trefoil-like filament, which encompasses a smaller closed filament within it. Both these filaments undergo individual curvature-dependent motion. The tiny enclosed filament rapidly gains a circular shape, shrinks in size [Figs. 5(d)–5(g)], and quickly disappears [Fig. 5(h)]. This detail can also be fleetingly observed in our experimental results (Fig. 2). The trefoil-shaped filament continues to slowly shrink, as it finally approaches a circular geometry and vanishes (shown later in Fig. 9).

V. DISCUSSIONS

Our numerical simulations for the two distinct arrangements of three scroll rings hinted at a difference in the lifetime of the scrolls. Figures 6(a) and 6(b) demonstrate how the total lifetime of the reconnected filament varies as a function of the geometry during interaction of three and four scroll rings, respectively. In the case of three rings, we have considered a

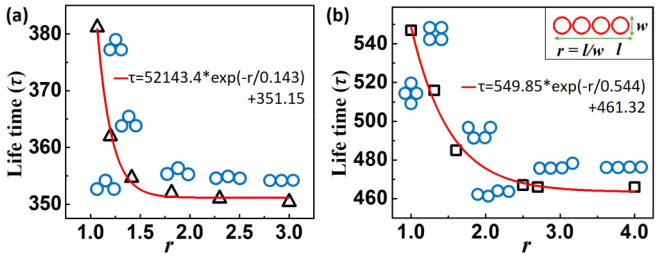

FIG. 6. Lifetime variation with change in geometry. The lifetimes (τ, in time units) of reconnected scrolls are plotted as a function of r for six different initial arrangements of (a) three scroll rings and (b) four scroll rings. Here r is defined as the ratio of length l to width w of the initial reconnected filament, where $l \geqslant w$, as shown in inset of (b). The corresponding arrangement of the scroll rings are shown next to each data point. In both the plots τ decreases exponentially with an increasing value of r.

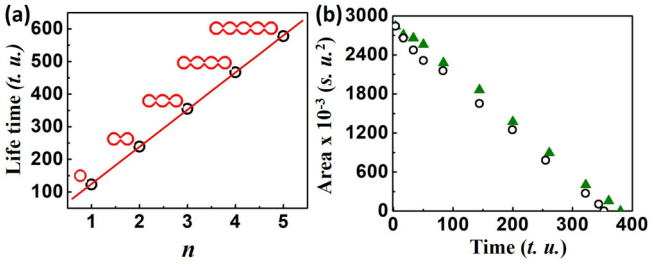

FIG. 7. (a) Lifetime as a function of number of rings that reconnect linearly. (b) Area enclosed by the filament as a function of time. Simulation results for three initial scroll rings placed in two different arrangements. Black open circles represent linear arrangement (as in Fig. 4) while green triangles represent a triangular arrangement (as in Fig. 5) of the scrolls.

total of six geometries, which fall between the two extreme cases (linear and equilateral triangle). We slowly varied the angle that the lines joining the centers of the three rings make. For a comparison of the lifetimes, we choose the aspect ratio r, the ratio of the length (the longer side) of the initial arrangement of rings to its width (the shorter side) as a measure of the geometry. The aspect ratio for the linear arrangement is 3.0, while for the equilateral triangle it is 1.07. For the intermediate arrangements of the circles, we have ratios of 2.3, 1.82, 1.41, and 1.2, respectively. When we plot the lifetimes of these reconnected filaments against r, we find an exponential curve that decays with increase in r. We then carried out simulations for six different configurations of four scroll rings. We chose the linear geometry ($r = 4.0$), square or quatrefoil geometry ($r = 1.0$) and in between them an elongated quatrefoil or rhomboidal geometry ($r = 1.3$), a trapezoidal geometry ($r = 1.6$), and two other arrangements with $r = 2.5$ and $r = 2.7$. Even for these configurations of the initial four scroll rings, the lifetimes decay exponentially with r.

A comparison of the lifetimes of reconnected filaments formed by n scroll rings whose centers are collinear is shown in Fig. 7(a). It is seen that the lifetime varies linearly as an increasing function of n. The difference in lifetimes for reconnected filaments of different geometries, but formed from initially the same number of concentric rings, require more attention. We calculated the area enclosed by the filaments for the simulations presented in Figs. 4 and 5. Both simulations initially had three circular filaments of the same size. Hence the total area enclosed by these filaments are exactly equal at time zero [Fig. 7(b)]. As time progresses and the filaments start to reconnect, the area enclosed under the triangular filament diverges slightly from the linear one. This happens at around 30 time units, or after five rotations (time period of one rotation is 5.4 time units), when the trefoil-shaped filament seems to stabilize for a while. After this the two filaments shrink, as the area enclosed under them decays, tracing almost parallel curves. The time required for the two filaments to completely disappear, or their lifetime, thus varies by about 30 time units in this case.

In our experiments, we tried to compare the two geometries of three initial scroll rings for the purpose of generating a similar graph of area as a function of time (Fig. 8). There

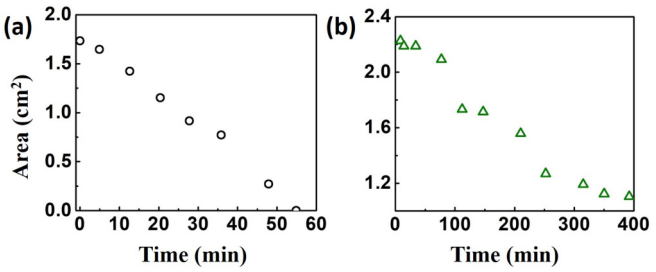

FIG. 8. Area enclosed by the filament as a function of time for two configurations of three scroll rings in an experimental BZ system. (a) Scrolls placed linearly as in Fig. 1. (b) Triangular arrangement of scrolls as in Fig. 2.

were, however, practical limitations to this. First, we were unable to get exact same sizes of the initial filaments, as that is extremely sensitive to environmental conditions. Second, as the reconnected filaments were quite large in size (as compared to single scroll waves), their lifetime increases tremendously. Meanwhile, as the reaction progresses, CO_2 bubbles that are generated during the reaction act as pinning sites for the filament. This happens during most experiments, and once the filament is anchored, it ceases to shrink or shrinks at a rather low pace. In Fig. 8, we show examples of two experiments that are similar to the ones seen in Fig. 1 and Fig. 2. The area enclosed by the reconnected filament for the linear case [Fig. 8(a)] is initially 1.75 cm^2 and is seen to decay as theoretically predicted. In the case of the triangular arrangement, we are able to observe the stabilization of the filament at around 35 mins after the initiation of the experiment [Fig. 8(b)]. This time corresponds to the fifth rotation of the vortex (time period 7 mins). This observation is consistent with that predicted by our numerical simulations. The area enclosed by the filament at this instant is around 2.0 cm^2, and it starts decaying. However, we observe that the filament seems to get stabilized again, beyond 300 min. After 6 h of experiment time, the system is full of CO_2 bubbles, and this is the reason that the filament gets pinned onto them, which arrests its further shrinkage.

In order to understand the reason for the difference in shrinkage behavior of the two filaments (linear and trefoil shaped) observed both in our experiments as well as numerical simulations, we look at the evolution of the filaments in the two cases under consideration (Fig. 9). The first noticeable difference between the two geometries is the area under the initially reconnected filament. While for the linear arrangement of scroll rings, the area is almost equal to the sum total of the three constituting circles [Fig. 9(a)], for the triangular arrangement, there is an extra area engulfed between the three circles, which gets included within the larger trefoil-shaped filament [Figs. 9(f) and 9(g)]. Second, the overall shape of the reconnected filaments in both the cases are very different. While, the former has a cylindrical shape like a dumbbell having three lobes instead of two, the latter has a trefoil-like geometry. The extended dumbbell has its own sets of concave and convex areas, which smoothen out to form a "hot dog"–shaped filament after about 29 rotations [Fig. 9(c)]. The hot dog shape can be considered to be a composite of two hairpins facing each other. These are shape-conserving

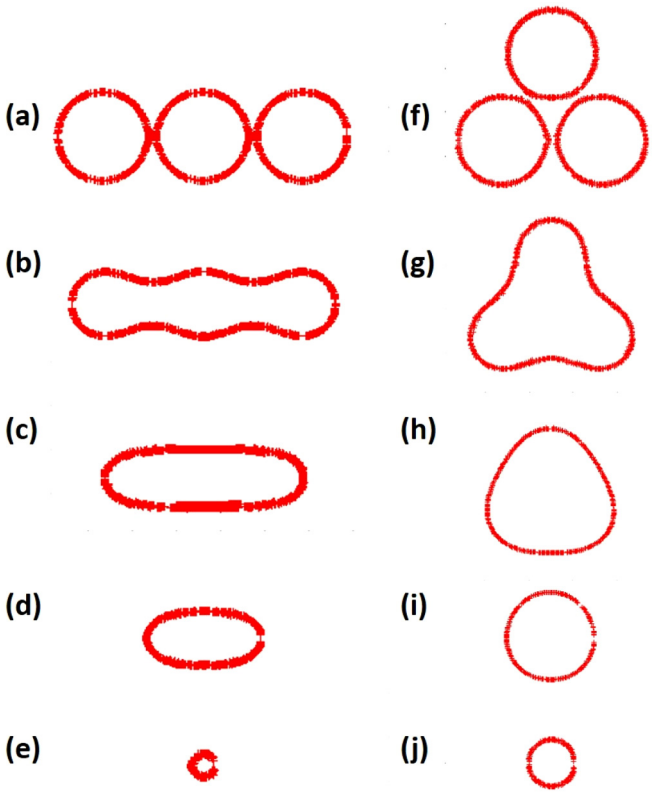

FIG. 9. Time evolution of filaments. These results have been generated from two numerical simulations. Filaments are shown at [(a) and (f)] 9 time units, [(b) and (g)] 57 time units, [(c) and (h)] 155 time units, and [(d) and (i)] 347 time units, after the initiation of the waves. [(a)–(e)] Linear arrangement of three scroll rings that evolve into a hot dog–shaped filament. [(f)–(j)] Triangular placement of initial filaments, leading to a trefoil-shaped vortex.

geometries [16,27] and they maintain their shapes as the two halves travel toward each other [Fig. 9(d)], with a constant velocity proportional to the width of the hot dog–shaped filament. Finally, after 64 rotations, the filament collapses as a tiny circle [Fig. 9(e)]. The trefoil-shaped filament, on the other hand, slowly gains a shape like a rounded Reuleaux triangle after about 29 rotations [Fig. 9(h)]. This further undergoes curvature-dependent flow and gains a circular shape [Fig. 9(i)] that shrinks with a velocity inversely proportional to the radius of the circle [27]. The relative velocity of shrinking of the two shapes (circular versus hot dog shaped) are also quite different [32]. These two causes result in a marked difference in the lifetime of the two reconnected filaments, starting from identical scroll rings.

VI. CONCLUSIONS

In this paper, we have demonstrated how multiple scroll-wave filaments undergo reconnection to form large filaments of complex geometry. When these scrolls lie sufficiently close to one another, within a specific range of interfilament distance, their filaments undergo crossover collision and merge after one or more cycles of individual rotation of the scrolls. The reconnected waves may have substantially large filaments of different irregular geometries in the initial

stage following reconnection. Due to the curvature-dependent behavior, the complex shapes of the reconnected filaments smoothen and gradually approach a regular geometry. The positive tension of the filaments make them shrink with time and finally collapse. It has been observed that the reconnected filaments have elongated lifetimes that could be many times the multiple of the independent scroll waves. Moreover, an equal number of scroll waves in the same excitable medium may reconnect in several ways to give rise to filaments having noticeably different lifetimes. We have theoretically studied various possible configurations for same number of scrolls (n) in detail and shown that the lifetime depends on the initial arrangement of the reconnecting scrolls. We propose that there exists a relationship between the aspect ratio of the filament geometries and their lifetimes. Extensive investigation has revealed that for any value of n, a linear arrangement of the reconnecting scroll waves has the lowest lifetime among all the possible geometries, which again is a linearly increasing function of n. An analysis of the variation of area enclosed by the filaments with time has helped us gain better insight into the influence of the initial geometrical configuration on the dynamics of the reconnected filament.

Further studies can be carried out to investigate the curvature-dependent flow dynamics of the reconnected filaments and it may be possible to deduce an exact mathematical relationship between their lifetime and geometries. It will also be interesting to study the nature of filament interaction around unexcitable heterogeneities. We hope that the results obtained in this work will provide newer insights into the behavior of scroll waves found in close vicinity of each other in other biological systems, such as the myocardial tissues of the heart.

ACKNOWLEDGMENT

This work was partially supported by the Science and Engineering Research Board, Government of India (Grant No. SB/S1/PC-19/2012).

[1] R. Kapral and K. Showalter, *Chemical Waves and Patterns* (Springer, Amsterdam, 1995).
[2] I. R. Epstein and J. A. Pojman, *An Introduction to Nonlinear Chemical Dynamics: Oscillations, Waves, Patterns, and Chaos* (Oxford University Press, New York, 1998).
[3] S. C. Müller, P. J. Plath, G. Radons, and A. Fuchs, *Complexity and Synergetics* (Springer International, Cham, 2018).
[4] Y. Yu, L. M. Santos, L. A. Mattiace, M. L. Costa, L. C. Ferreira, K. Benabou, A. H. Kim, J. Abrahams, M. V. L. Bennett, and R. Rozental, Proc. Natl. Acad. Sci. USA **109**, 2585 (2012).
[5] X. Huang, W. Troy, Q. Yang, H. Ma, C. Laing, S. Schiff, and J. Y. Wu, J. Neurosci. **24**, 9897 (2004).
[6] J. Lechleiter, S. Girard, E. Peralta, and D. Clapham, Science **252**, 123 (1991).
[7] O. Steinbock, F. Siegert, S. C. Müller, and C. J. Weijer, Proc. Natl. Acad. Sci. USA **90**, 7332 (1993).
[8] A. T. Winfree, Science **266**, 1003 (1994).
[9] F. H. Fenton, E. M. Cherry, H. M. Hastings, and S. J. Evans, Chaos **12**, 852 (2002).
[10] R. A. Gray, J. Jalife, A. V. Panfilov, W. T. Baxter, and C. Cabo, Science **270**, 1222 (1995).
[11] J. P. Keener, Physica D **34**, 378 (1989).
[12] J. P. Keener and J. J. Tyson, SIAM Rev. **34**, 1 (1992).
[13] J. Jalife, M. Delmar, J. Anumonwo, O. Berenfeld, and J. Kalifa, *Basic Cardiac Electrophysiology for the Clinician*, 2nd ed. (Wiley-Blackwell, Oxford, UK, 2009).
[14] A. T. Winfree and S. H. Strogatz, Physica D **8**, 35 (1983).
[15] A. V. Panfilov, R. R. Aliev, and A. V. Mushinsky, Physica D **36**, 181 (1989).
[16] J. P. Keener and J. J. Tyson, Science **239**, 1284 (1988).
[17] M. Vinson, S. Mironov, S. Mulvey, and A. Pertsov, Nature (London) **386**, 477 (1997).
[18] N. P. Das and S. Dutta, Phys. Rev. E **96**, 022206 (2017).
[19] D. Kupitz and M. J. B. Hauser, J Phys. Chem. A **117**, 12711 (2013).
[20] N. P. Das and S. Dutta, Phys. Rev. E **91**, 030901(R) (2015).
[21] J. Schutze, O. Steinbock, and S. C. Müller, Nature (London) **356**, 45 (1992).
[22] V. I. Krinsky and K. I. Agladze, Physica D **8**, 50 (1983).
[23] M. Vinson, Physica D **116**, 313 (1998).
[24] B. Fiedler and R. M. Mantel, Doc. Math. **5**, 695 (2000).
[25] M-A. Bray and J. P. Wikswo, Phys.Rev. Lett. **90**, 238303 (2003).
[26] R. H. Clayton and A. V. Holden, Phys. Med. Biol. **47**, 1777 (2002).
[27] T. Bánsági, Jr. and O. Steinbock, Phys. Rev. Lett. **97**, 198301 (2006).
[28] See Supplemental Material at http://link.aps.org/supplemental/10.1103/PhysRevE.100.022222, for movies of experiments and additional experimental and numerical data.
[29] P. M. Sutcliffe and A. T. Winfree, Phys. Rev. E **68**, 016218 (2003).
[30] D. Barkley, Physica D **49**, 61 (1991).
[31] Michael Seipel, Friedemann W. Schneider, and Arno F. Münster, Faraday Discuss. **120**, 395 (2002).
[32] S. Dutta and O. Steinbock, Phys. Rev. E **81**, 055202(R) (2010).